Diabetologia (2018) 61:906–918
https://doi.org/10.1007/s00125-017-4542-6

ARTICLE

SIRT6-mediated transcriptional suppression of *Txnip* is critical for pancreatic beta cell function and survival in mice

Kunhua Qin[1,2] · Ning Zhang[3] · Zhao Zhang[1] · Michael Nipper[2] · Zhenxin Zhu[2] · Jake Leighton[2] · Kexin Xu[1] · Nicolas Musi[3] · Pei Wang[2]

Received: 6 July 2017 / Accepted: 4 December 2017 / Published online: 10 January 2018

Abstract

Aims/hypothesis Better understanding of how genetic and epigenetic components control beta cell differentiation and function is key to the discovery of novel therapeutic approaches to prevent beta cell dysfunction and failure in the progression of type 2 diabetes. Our goal was to elucidate the role of histone deacetylase sirtuin 6 (SIRT6) in beta cell development and homeostasis.

Methods *Sirt6* endocrine progenitor cell conditional knockout and beta cell-specific knockout mice were generated using the Cre-*loxP* system. Mice were assayed for islet morphology, glucose tolerance, glucose-stimulated insulin secretion and susceptibility to streptozotocin. Transcriptional regulatory functions of SIRT6 in primary islets were evaluated by RNA-Seq analysis. Reverse transcription-quantitative (RT-q)PCR and immunoblot were used to verify and investigate the gene expression changes. Chromatin occupancies of SIRT6, H3K9Ac, H3K56Ac and active RNA polymerase II were evaluated by chromatin immunoprecipitation.

Results Deletion of *Sirt6* in pancreatic endocrine progenitor cells did not affect endocrine morphology, beta cell mass or insulin production but did result in glucose intolerance and defective glucose-stimulated insulin secretion in mice. Conditional deletion of *Sirt6* in adult beta cells reproduced the insulin secretion defect. Loss of *Sirt6* resulted in aberrant upregulation of thioredoxin-interacting protein (TXNIP) in beta cells. SIRT6 deficiency led to increased acetylation of histone H3 lysine residue at 9 (H3K9Ac), acetylation of histone H3 lysine residue at 56 (H3K56Ac) and active RNA polymerase II at the promoter region of *Txnip*. SIRT6-deficient beta cells exhibited a time-dependent increase in H3K9Ac, H3K56Ac and TXNIP levels. Finally, beta cell-specific SIRT6-deficient mice showed increased sensitivity to streptozotocin.

Conclusions/interpretation Our results reveal that SIRT6 suppresses *Txnip* expression in beta cells via deacetylation of histone H3 and plays a critical role in maintaining beta cell function and viability.

Data availability Sequence data have been deposited in the National Institutes of Health (NIH) Gene Expression Omnibus (GEO) with the accession code GSE104161.

Keywords Beta cell · Diabetes · H3K9Ac · Insulin secretion · SIRT6 · TXNIP

Electronic supplementary material The online version of this article (https://doi.org/10.1007/s00125-017-4542-6) contains peer-reviewed but unedited supplementary material, which is available to authorised users.

✉ Pei Wang
wangp3@uthscsa.edu

[1] Department of Molecular Medicine, University of Texas Health Science Centre at San Antonio, San Antonio, TX, USA

[2] Department of Cell Systems & Anatomy, University of Texas Health Science Centre at San Antonio, 7703 Floyd Curl Drive, San Antonio, TX 78229-3900, USA

[3] Barshop Institute for Longevity and Aging Studies, University of Texas Health Science Centre at San Antonio, San Antonio, TX, USA

Abbreviations

BKO	Beta cell-specific knockout
ChIP	Chromatin immunoprecipitation
EKO	Endocrine pancreas-specific knockout
HAT	Histone acetyltransferase
HDAC	Histone deacetylase
H3K9Ac	Acetylation of histone H3 lysine residue at 9
H3K18Ac	Acetylation of histone H3 lysine residue at 18
H3K56Ac	Acetylation of histone H3 lysine residue at 56
MIP1-CreER	Mouse insulin promoter 1-driven, inducible CreERT transgenic line
NGN3	Neurogenin 3
NIH	National Institutes of Health

Research in context

What is already known about this subject?

- The NAD^+-dependent deacetylase sirtuin 6 (SIRT6) is essential for normal animal development
- Mice deficient for SIRT6 develop multiple growth and metabolic defects
- SIRT6 is closely associated with chromatin and works as a transcriptional co-suppressor by catalysing the deacetylation of histone H3 lysine residues acetylated at positions 9, 56 and 18

What is the key question?

- What is the role of SIRT6 in beta cell development and homeostasis?

What are the new findings?

- SIRT6 maintains an adequate level of H3K9Ac and H3K56Ac in beta cells
- SIRT6 controls glucose-stimulated insulin secretion in beta cells partially by inhibiting *Txnip* expression
- Long-term loss of histone deacetylase activity of SIRT6 in beta cells is associated with increased susceptibility to the diabetogenic agent streptozotocin

How might this impact on clinical practice in the foreseeable future?

- Stimulating SIRT6 activity and expression in beta cells could be beneficial for preserving insulin secretion and preventing the progression of diabetes

ROS	Reactive oxygen species
SIRT6	Sirtuin 6
STZ	Streptozotocin
TSS	Transcriptional start site
TXNIP	Thioredoxin-interacting protein

Introduction

Beta cells, the major cell type in the endocrine pancreas, control glucose homeostasis by secreting insulin in response to blood sugar level [1]. Dysfunction of beta cells and impaired insulin sensitivity of peripheral tissues lead to type 2 diabetes [2]. Histone modifications, including acetylation, methylation, phosphorylation and ubiquitination, affect the accessibility of genetic information by altering the physical interaction of DNA, histones and non-histone proteins [3]. Studies have shown that histone acetylation and deacetylation play pivotal roles in regulating endocrine differentiation and beta cell maturation and function [4]. In addition, histone acetylation and deacetylation are implicated in the pathogenesis of diabetes [5]. Thus, targeting such mechanisms may provide a potential approach to treat diabetes [5]. The biochemical reactions of histone acetylation and deacetylation in cells are executed by catalytic enzymes called histone acetyltransferases (HATs) and histone deacetylases (HDACs) [5]. Despite the identification of more than 20 HATs and 18 HDACs [6, 7], the expression pattern and precise function of these specific enzymes in beta cells are not yet fully understood. Furthermore, despite extensive studies conducted in vitro, the physiological functions of these proteins have not been completely established [8].

Sirtuins, first identified in yeast as ageing regulators, belong to the class III HDACs [9]. There are seven members in the mammalian sirtuin family (sirtuin 1–7) [9], all of which exhibit NAD-dependent deacetylation activity. However, different sirtuins act on different substrates and are localised in specific subcellular compartments [10]. For example, SIRT6 is closely associated with chromatin and works as a transcriptional co-suppressor by catalysing the deacetylation of histone H3 lysine residues acetylated at positions 9, 56 and 18 (H3K9Ac, H3K56Ac and H3K18Ac) [11–13]. Prior genetic studies showed that SIRT6 is essential for mouse development and plays versatile roles in regulating glucose homeostasis, lipid metabolism and many other processes [14]. To elucidate the role of SIRT6 in beta cell development and homeostasis, we generated endocrine pancreas-specific (EKO) and beta cell-specific knockout (BKO) mouse models in which *Sirt6* was deleted at the embryonic and adult stages, respectively. By taking advantage of transcriptome analysis, we further investigated the underlying mechanisms by which SIRT6 contributes to endocrine pancreas functions.

Methods

Animal studies All mouse studies were approved by the Institutional Animal Care and Use Committee of the

University of Texas Health Science Centre at San Antonio. The *Sirt6* flox/flox (f/f) [15], *Ngn3*-Cre [16] (*Ngn3* is also known as *Neurog3*) and mouse insulin promoter 1-driven, inducible CreERT transgenic line (MIP1-CreERT) [17] mice were obtained from the Jackson Laboratory (Bar Harbor, ME, USA) and maintained in a mix genetic background. Mice were housed in a conventional facility with a 12 h night–day cycle and free access to food and water. Mouse genotyping was performed using a dirty-tail method as previously described [18]. Tamoxifen (T5648; Sigma, St Louis, MO, USA) was used to delete the floxed *Sirt6* allele via the MIP1-CreERT system [19]. Male mice at 2–11 months old and female mice at 2–9 months old were used in the analysis. For all the experiments, *Sirt6* EKO mice or *Sirt6* BKO mice and their littermate control mice (see electronic supplementary material [ESM] Fig. 1a and ESM Fig. 4 for the breeding strategy) were selected by genotype and were randomly assigned a unique label in the tail, with the genotype blinding to operators until experiments were completed. No data were excluded in all the analysis. See ESM Table 1 and ESM Methods for genotyping primers and experimental procedures for tamoxifen injection, verapamil (V4629; Sigma) treatment and streptozotocin (STZ) (S0130; Sigma) challenge.

Changes in pancreas and islet architecture were revealed by H&E staining and anti-insulin, anti-glucagon and anti-somatostatin immunostaining. Beta cell apoptosis was determined by anti-cleaved caspase 3 immunostaining. The metabolic studies, including glucose measurement, insulin measurement, IPGTT, ITT and hyperglycaemic clamp were performed as previously reported [20]. See ESM Methods for details.

Pancreatic islet isolation and glucose-stimulated insulin secretion Islets were isolated by collagenase perfusion and used for determination of glucose-stimulated insulin secretion as previously described [21]. See ESM Methods for details.

Gene expression *Sirt6* mRNA levels in *Ngn3*-null and *Ngn3*-positive cells at mouse embryonic day 15.5 (E15.5) were generated using data from Table S6 in Benitez et al [22]. *Sirt6* and *Txnip* mRNA levels in isolated islets were determined by reverse transcription (RT) quantitative (q)-PCR. See ESM Methods for details.

Immunoblotting SIRT6, thioredoxin-interacting protein (TXNIP), H3K9Ac, H3K27Ac and H3K56Ac levels were determined by immunoblotting. See ESM Methods for details.

RNA-Seq analysis Islets isolated from 2 weeks post-tamoxifen control ($Sirt6^{f/+}$; MIP1-CreERT) and *Sirt6* BKO ($Sirt6^{f/f}$; MIP1-CreERT) mice and 2-month-old control ($Sirt6^{+/+}$; *Ngn3*-Cre or $Sirt6^{f/f}$) and *Sirt6* EKO ($Sirt6^{f/f}$; *Ngn3*-Cre) mice were used for the RNA-Seq analysis. See ESM Methods for details.

ChIP Chromatin occupancies of SIRT6, IgG, H3K9Ac, H3K56Ac and Active RNA polymerase II in beta cells were determined by chromatin immunoprecipitation (ChIP) [23]. See ESM Methods for details.

Statistical analysis All results are presented as means ± SEM. Statistical analysis was performed by two-tailed Student's *t* test. p values <0.05 were considered statistically significant.

Results

Deletion of *Sirt6* in pancreatic endocrine progenitor cell does not affect beta cell development Gene expression profiles of pancreatic cells throughout different stages of mouse pancreas development were analysed previously [22]. Using the data from this study (Table S6) we found that *Sirt6* transcripts were expressed at a much higher level in E15.5 neurogenin 3 (NGN3)-expressing endocrine progenitor cells than in *Ngn3*-null cells (Fig. 1a) [22]. In the adult mouse pancreas, *Sirt6* transcripts and proteins were also expressed highly in isolated islets (Fig. 1b, d). To examine the role of SIRT6 in endocrine pancreas development and function, we generated an EKO mouse model ($Sirt6^{f/f}$; *Ngn3*-Cre) by crossing $Sirt6^{f/f}$ mice with the *Ngn3*-Cre strain (ESM Fig. 1a) [24]. As expected, the *Sirt6* transcripts and proteins were undetectable in islets isolated from mutant mice (Fig. 1c, d), indicating efficient deletion of the *Sirt6* gene in the endocrine pancreas.

The EKO mice were born at the expected Mendelian ratio and displayed no overt phenotype. To test whether loss of *Sirt6* affects endocrine morphology, we collected pancreases from 2-month-old control and EKO mice and performed histological analysis. No obvious differences between the pancreases of the two groups were revealed by H&E staining (data not shown). Furthermore, immunostaining for insulin and glucagon showed no apparent changes in islet architecture or islet number (Fig. 1e, f and ESM Fig. 1b). Endocrine cell mass analysis showed no change in beta cell mass in EKO mouse pancreases (Fig. 1g). However, alpha cell mass showed a decrease (not statistically significant) and delta cell mass showed a statistically significant increase (ESM Fig. 1c, d). These data are consistent with the results reported from recent studies in which *Sirt6* was knocked out in early pancreas and beta cells [25, 26]. Thus, deletion of *Sirt6* in NGN3-expressing progenitor cells does not affect beta cell development or endocrine pancreas gross morphology.

Deletion of *Sirt6* in pancreatic endocrine progenitor cell leads to defective glucose-stimulated insulin secretion Next, we assessed the effect of *Sirt6* knockout on glucose homeostasis function of the endocrine pancreas. During fasting or feeding, blood glucose and plasma insulin levels of mutant mice were comparable with those of their littermate controls (Fig. 2a, b).

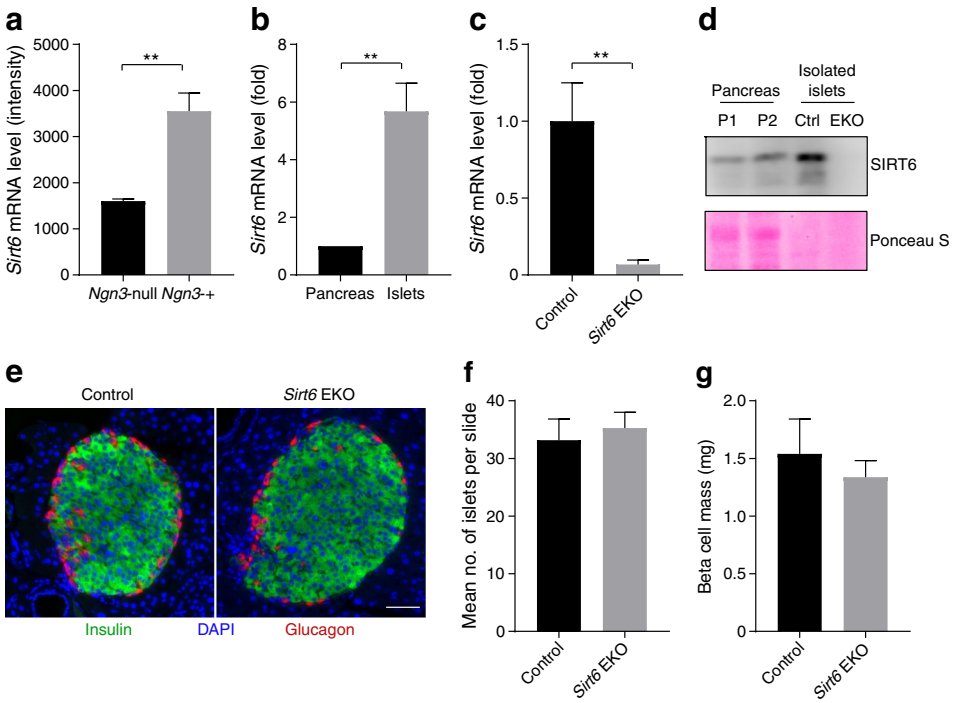

Fig. 1 Deletion of *Sirt6* in pancreatic endocrine progenitor cells does not affect beta cell development. (**a**) *Sirt6* mRNA levels in E15.5 *Ngn3*-null cells and *Ngn3*-positive cells, $n = 3$–4; the graph was generated based on data published previously [22]. (**b**) RT-qPCR of *Sirt6* mRNA levels in the pancreas and isolated islets. The relative expression level of *Sirt6* mRNA in islets was normalised to that in the pancreas, $n = 3$. (**c**) RT-qPCR of *Sirt6* mRNA levels in islets from the control ($Sirt6^{f/f}$) and *Sirt6* EKO mice, $n = 3$. (**d**) Immunoblot of SIRT6 protein in the pancreas or islets isolated from the control and *Sirt6* EKO mice. P1, P2, pancreas samples from two separate control mice ($Sirt6^{f/f}$). (**e**) Immunostaining of pancreatic islets (green: anti-insulin; blue, DAPI; red, anti-glucagon) from control and *Sirt6* EKO mice. Scale bar, 50 μm. (**f**, **g**) Quantification of the average number of islets per section (**f**) and beta cell mass (**g**), $n = 3$ in control and *Sirt6* EKO mice. Data are expressed as means ± SEM. $^{**}p < 0.01$ for indicated comparisons

However, an IPGTT revealed a severe glucose intolerance phenotype in 2- to 3-month-old *Sirt6* EKO mice (Fig. 2c, d and ESM Fig. 2a, b). We found that insulin levels during the IPGTT were significantly lower in the *Sirt6* EKO mice than in control mice at 15 min (Fig. 2e), implying that the defect in the EKO mice may be due to insulin insufficiency. Moreover, we found that the glucose intolerance phenotype became more severe in 5- to 6-month-old *Sirt6* EKO mice, as indicated by the AUC of the GTT, which increased from 147% to 205% of the control value (Fig. 2d, g and ESM Fig. 2c, d), suggesting that the phenotype worsened over time. An ITT showed that in mice aged 8–10 months, the response to insulin of peripheral tissues was the same in *Sirt6* EKO mice as in control mice (ESM Fig. 3), further pointing to defective insulin production or secretion as being the cause of the impaired glucose tolerance [27]. *Sirt6* EKO mouse pancreases had normal total insulin content (Fig. 3a). Thus, our data supported the notion that the phenotype was caused by an insulin secretion defect of the endocrine pancreas. To test this, we isolated islets from the mice and performed a glucose-stimulated insulin secretion assay in vitro. As expected, upon incubation with a high concentration of glucose, the amount of insulin released from *Sirt6* EKO cells was only one-third of that release by cells from control mice (Fig. 3b). Furthermore, during a hyperglycaemic clamp procedure to evaluate beta cell function in vivo, we observed that *Sirt6* EKO mice required a significantly lower glucose infusion rate to maintain the glucose level at approximately 16 mmol/l (Fig. 3c, d), and that plasma insulin concentrations of EKO mice were much lower than those of their control littermates (Fig. 3e, f). Thus, combined in vitro and in vivo results illustrate that deletion of *Sirt6* in the endocrine pancreas leads to defective glucose-stimulated insulin secretion.

Beta cell-specific *Sirt6* knockout leads to defective insulin secretion Given the fact that NGN3 progenitor cells generate other cell types besides beta cells during development [22], we sought to determine whether the *Sirt6* EKO phenotype was intrinsic to beta cells. To this end, we generated *Sirt6* BKO mice, with beta cell-specific *Sirt6* deletion, by intercrossing the floxed *Sirt6* mice with MIP1-CreERT mice (ESM Fig. 4) [19]. Two weeks following tamoxifen treatment, SIRT6 transcript and protein levels in primary islets isolated from *Sirt6* BKO ($Sirt6^{f/f}$; MIP1-CreERT) mice were reduced to less than 20% of normal (Fig. 4a, b). The remaining signals were likely due to the expression of SIRT6 in alpha cells or other types of endocrine cells [8]. Similar to *Sirt6* EKO mice, *Sirt6* BKO mice had normal fasting and fed glucose levels (Fig. 4c) but displayed glucose intolerance

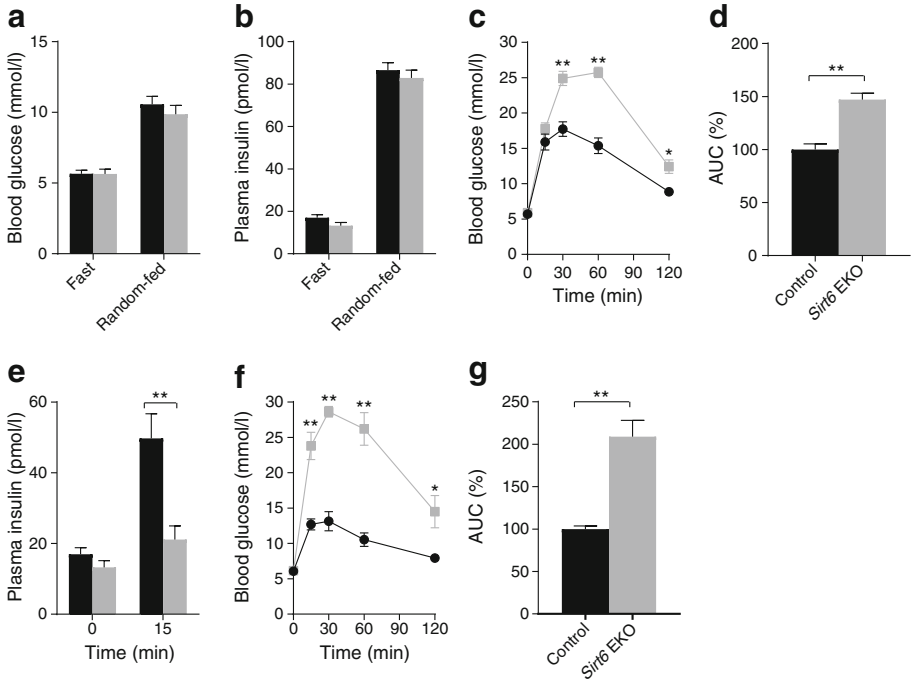

Fig. 2 Deletion of *Sirt6* in pancreatic endocrine progenitor cell leads to glucose intolerance. (**a**) Blood glucose levels of 2-month-old control (*Sirt6*$^{f/f}$) and *Sirt6* EKO male mice in the fasting or random-fed state ($n = 6$). (**b**) Plasma insulin levels of 2-month-old control and *Sirt6* EKO male mice in the fasting or random-fed state ($n = 5$). (**c**) Blood glucose after GTTs in 2- to 3-month-old male mice ($n = 8$ control; $n = 13$ EKO). (**d**) Normalised area under the GTT curve. (**e**) Plasma insulin levels of 2- to 3-month-old control and *Sirt6* EKO mice during the GTT ($n = 4$–6). (**f**) Glucose tolerance tests of 5- to 6-month-old male mice ($n = 4$ control; $n = 5$ EKO). (**g**) The normalised area under the GTT curve. Black bars and circles, control mice; grey bars and squares, *Sirt6* EKO mice. Data are expressed as means ± SEM. $^*p < 0.05$ and $^{**}p < 0.01$ vs control mice or for indicated comparisons

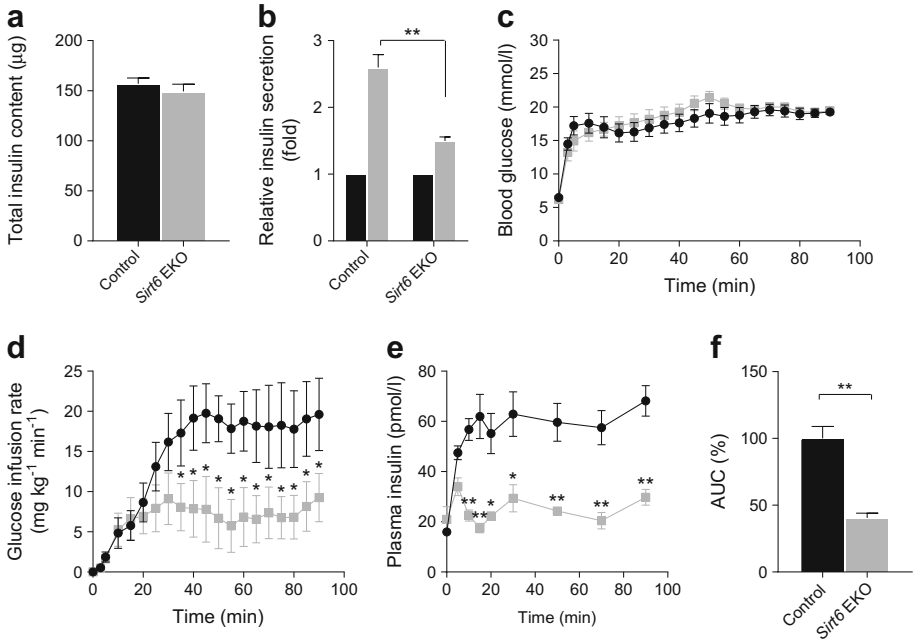

Fig. 3 Deletion of *Sirt6* in pancreatic endocrine progenitor cell leads to defective glucose-stimulated insulin secretion. (**a**) The total insulin content of the pancreas ($n = 3$ control; $n = 4$ EKO). (**b**) Relative insulin levels secreted from four pairs of islets isolated from control (*Sirt6*$^{f/f}$) and EKO mice treated with 16.7 mmol/l glucose for 1 h; values were normalised to those of the 2.5 mmol/l glucose treatment group. (**c**–**e**) Blood glucose levels (**c**), glucose infusion rates (**d**) and plasma insulin concentrations (**e**) of 4-month-old control and *Sirt6* EKO mice during the hyperglycaemic clamp assay ($n = 6$ control; $n = 7$ EKO). (**f**) The normalised AUC for plasma insulin concentration of the 4-month-old control and *Sirt6* EKO mice during the hyperglycaemic clamp assay. Black bars and circles, control mice; grey bars and squares, *Sirt6* EKO mice. Data are expressed as means ± SEM. $^*p < 0.05$ and $^{**}p < 0.01$ vs control mice or for indicated comparisons

because of insufficient insulin secretion (Fig. 4d–f). Notably, the insulin levels in *Sirt6* BKO mice at 0 min were lower than those in control mice, which was not observed in our *Sirt6* EKO mice (Fig. 2e), highlighting the difference between the two models. Moreover, in line with our observations made in *Sirt6* EKO mice of different ages, the glucose intolerance phenotype worsened over time in *Sirt6* BKO mice as well (Fig. 4g–j), further confirming that the phenotype was largely due to *Sirt6* deletion in beta cells. Together, these findings demonstrate that SIRT6 is required for glucose-stimulated insulin secretion in beta cells.

***Sirt6* knockout leads to aberrant upregulation of TXNIP** To gain mechanistic insight into how SIRT6 regulates glucose-stimulated insulin secretion, we analysed the transcriptomes of the islets isolated from control and mutant mice (two pairs of *Sirt6* BKO mice, 2 weeks post-tamoxifen and two pairs of *Sirt6* EKO mice, 2 months old) by RNA-Seq. Out of roughly 20,000 genes evaluated, a total of 99 and 243 genes were upregulated or downregulated more than 1.5-fold in the islets from *Sirt6* BKO mice and *Sirt6* EKO mice, respectively (GSE104161). In agreement with data shown in Fig. 3a, the levels of insulin-encoding mRNA (*Ins1* and *Ins2*) were comparable in control and mutant islets. Additionally, the

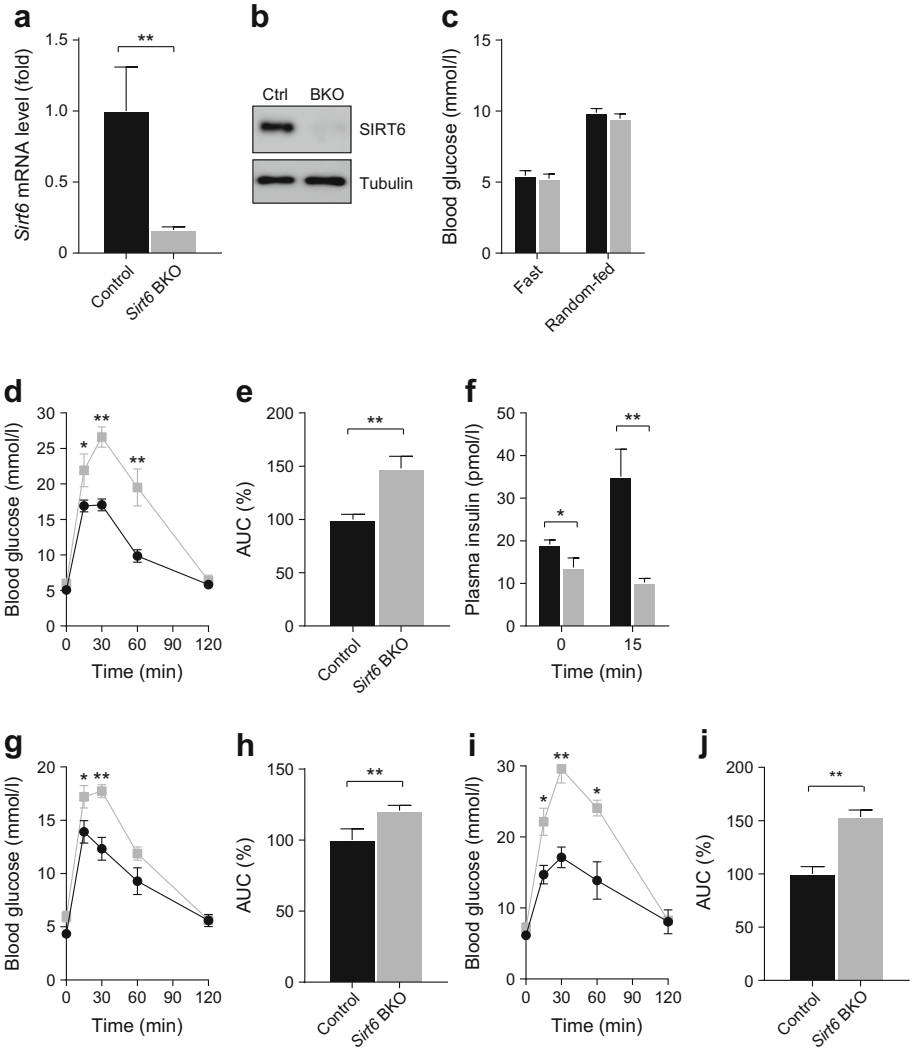

Fig. 4 Beta cell-specific deletion of *Sirt6* leads to defective insulin secretion. (**a**, **b**) RT-qPCR analysis of *Sirt6* mRNA (**a**) and immunoblots of SIRT6 expression (**b**) in islets isolated from control (Ctrl, a combination of MIP1-CreER and *Sirt6*$^{f/+}$; MIP1-CreER mice after tamoxifen treatment) and *Sirt6* BKO mice 2 weeks after deletion ($n = 3$). (**c**) Fasting and random-fed blood glucose levels of the 2 weeks post-tamoxifen (2-month-old) control and *Sirt6* BKO male mice ($n = 5$–6). (**d**) Blood glucose during GTTs in 2 weeks post-tamoxifen (2-month-old) control and *Sirt6* BKO male mice ($n = 5$ or 6). (**e**) AUC for blood glucose levels during GTT shown in (**d**). (**f**) Plasma insulin levels in the 2 weeks post-tamoxifen (2-month-old) control and *Sirt6* BKO mice during the GTT, related to (**d**) ($n = 4$). (**g**, **h**) Blood glucose levels during GTTs (**g**) and normalised AUCs (**h**) in 2 weeks post-tamoxifen control and *Sirt6* female BKO mice ($n = 4$). (**i**, **j**) Blood glucose levels during GTTs (**i**) and normalised AUCs (**j**) in 4 months post-tamoxifen control and *Sirt6* BKO female mice ($n = 4$ control; $n = 5$ BKO). Black bars and circles, control mice; grey bars and squares, *Sirt6* BKO mice. Data are expressed as means ± SEM. $^{*}p < 0.05$ and $^{**}p < 0.01$ vs control mice or for indicated comparisons

expression levels of genes associated with the occurrence of maturity-onset diabetes of the young or type 2 diabetes, such as *Pdx1*, *Hnf4a* and *Neurod1*, were unaltered in mutant islets [1].

To our surprise, only a subset of 23 genes showed a similar trend in both models: 18 were upregulated and 5 were downregulated (Fig. 5a, b). Nevertheless, a hypergeometric probability test revealed that this overlap was highly significant ($p < 1.96 \times 10^{-10}$; Fig. 5a). Among the upregulated genes in mutant islets, *Txnip* encodes a ubiquitous thioredoxin-binding protein that suppresses the antioxidant activity of thioredoxin, which is essential for eliminating reactive oxygen species (ROS) in cells [28]. It has been reported that TXNIP expression is negatively associated with glucose-stimulated insulin secretion in beta cells and that overexpression of TXNIP inhibits insulin secretion [29–31]. To test the hypothesis that TXNIP mediated the insulin secretion defect in the *Sirt6* KO beta cells, we first validated the change in TXNIP expression in SIRT6-deficient islets by immunoblot. As expected, TXNIP protein levels were significantly upregulated in islets isolated from 3-month-old *Sirt6* EKO mice (Fig. 5c, d). Simultaneously, we also detected a higher level of H3K9Ac in the *Sirt6* EKO islets (Fig. 5c), reflecting that loss of the histone deacetylation function of SIRT6 was correlated with elevated expression of *Txnip*.

Verapamil has been shown to repress *Txnip* transcription [32]. We tested whether reducing TXNIP levels by verapamil could partially rescue the impaired glucose tolerance in SIRT6-deficient mice (ESM Fig. 5a). After three weeks oral verapamil treatment (100 mg/kg per day), the immunoblot analysis showed that islets isolated from the two groups expressed similar levels of TXNIP, yet islets from *Sirt6* EKO mice still had higher H3K9Ac levels (ESM Fig. 5d). Consistent with the previous findings [32], verapamil lowered the overall glucose level in both control and *Sirt6* EKO mice at 8–9 months old (ESM Fig. 5b, f). Analysis of blood glucose during a GTT showed that the *Sirt6* EKO mice manifested largely restored tolerance to glucose (ESM Fig. 5e, f). Indeed, five out of six *Sirt6* EKO mice showed a similar response to that of control mice. Concurrently, plasma insulin levels of verapamil-treated *Sirt6* EKO mice increased 1.5-fold at 15 min after glucose challenge (ESM Fig. 5h, $p = 0.05$). Note that plasma insulin levels of verapamil-treated control mice increased 1.8-fold and that there was no increase in *Sirt6* EKO mice before verapamil treatment (ESM Fig. 5h, d). Together, these data suggest that verapamil treatment partially restored glucose-stimulated insulin secretion in *Sirt6* EKO mice, indicating that TXNIP is likely a mediator of the insulin secretion defect in SIRT6-deficient beta cells.

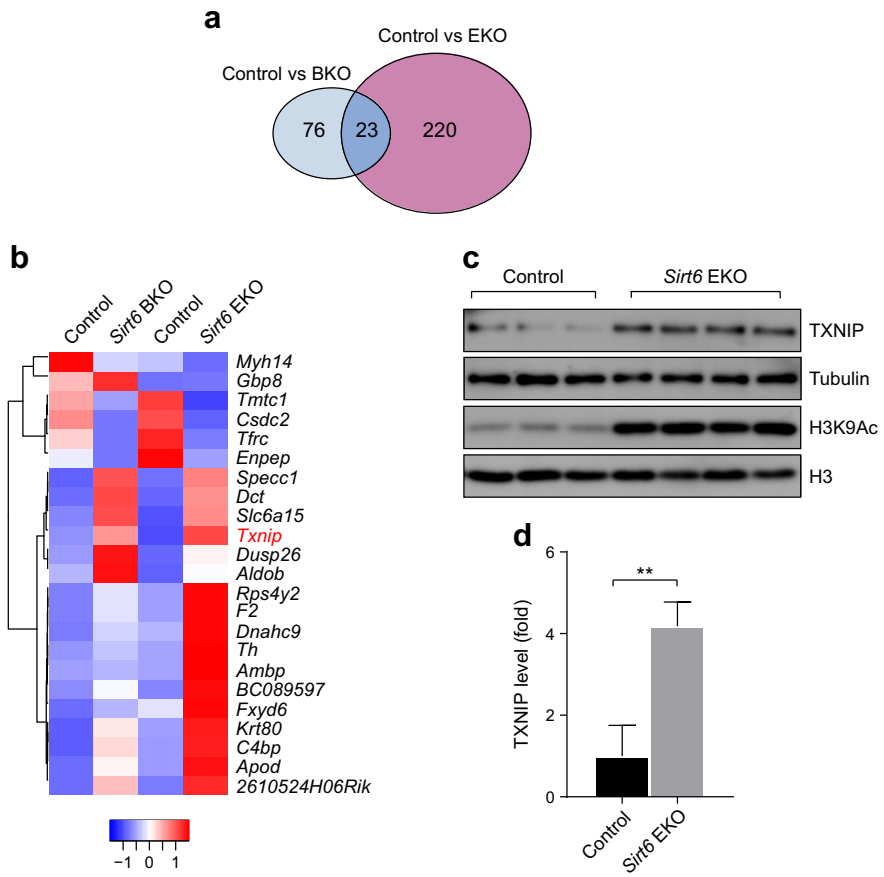

Fig. 5 Loss of SIRT6 leads to upregulation of TXNIP. (**a**, **b**) Venn diagram (**a**) and heat map (**b**) of the overlapped genes between the two *Sirt6* KO models from the RNA-Seq analysis. $p < 1.96 \times 10^{-10}$. (**c**, **d**) Immunoblots and quantification (**d**) of TXNIP expression levels in islets from 3-month-old control (*Sirt6*$^{f/f}$) and *Sirt6* EKO mice. Data are expressed as means ± SEM ($n = 3$–4). $^{**}p < 0.01$ for indicated comparison

SIRT6 regulates both basal and glucose-induced *Txnip* transcription As glucose is a potent inducer of TXNIP [33], we next examined the influence of SIRT6 deficiency on glucose-induced *Txnip* transcription. To this end, we isolated islets from overnight fasted mice and cultured them in serum-free medium with 2.5 mmol/l glucose. Note that this concentration is lower than the fasting glucose concentration in vivo (~5 mmol/l). Interestingly, we found that in this condition, *Txnip* mRNA levels in islets isolated from 3-month-old *Sirt6* EKO mice were 1.5-fold higher than those in control islets (Fig. 6a), suggesting that there was a basal upregulation of TXNIP in the mutant islets. Upon incubation of control islets with 16.7 mmol/l glucose for 1 h, *Txnip* mRNA levels increased 1.5-fold and reached the level found in *Sirt6* EKO islets in the basal condition (Fig. 6a). In contrast, high glucose treatment of *Sirt6* EKO islets induced a 3.3-fold increase in *Txnip* mRNA beyond its higher basal level (Fig. 6a). TXNIP immunoblot showed consistent results (Fig. 6b, c). These data support the idea that SIRT6 suppresses both basal and glucose-induced TXNIP expression in normal beta cells. In addition, we found that the acute glucose treatment did not affect upregulated H3K9Ac levels in the mutant islets (Fig. 6b). Together, these findings suggest that loss of *Sirt6* leads to impaired regulation of TXNIP in beta cells.

SIRT6 directly regulates *Txnip* by controlling H3K9Ac and H3K56Ac levels To determine whether *Txnip* is directly regulated by SIRT6, we examined chromatin occupancy of SIRT6 at the *Txnip* promoter region by ChIP. SIRT6-positive signals were highly enriched at the transcriptional start site (TSS) of *Txnip*, compared with the region 2 kb upstream of the *Txnip* TSS (−2 kb) (Fig. 7a, b). *Cis*-regulatory elements of the *Txnip* gene are near its TSS (−169 bp to −73 bp) [34]. Thus, this result indicates that SIRT6 is mainly located in the active transcription region of its target, consistent with a previous SIRT6 ChIP-seq study [35].

To further clarify how SIRT6 regulates *Txnip* expression, we analysed several SIRT6-catalysed histone H3 modifications by immunoblot [14]. *Sirt6* EKO mouse islets expressed a significantly higher level of H3K9Ac and H3K56Ac compared with control mouse islets (Fig. 7c–e). In contrast, the level of another histone H3 modification, H3K27Ac, which has been linked to SIRT6 deacetylation activity in vitro [14], was similar in control and EKO islets (Fig. 7f, g). These results show that loss of SIRT6 leads to an aberrant global increase in H3K9Ac and H3K56Ac in beta cells.

Next, we compared H3K9Ac and H3K56Ac ChIP signals at the local promoter regions of *Txnip* in islets isolated from 3-month-old control and *Sirt6* EKO mice under normal feeding. Consistent with the reported role of H3K9Ac and H3K56Ac in transcriptional activation and our earlier SIRT6 ChIP data, we detected significant enrichment of both markers at the TSS of the *Txnip* gene in the control islets. After loss of SIRT6, the H3K9Ac level at the TSS was further elevated around twofold, whereas it was unaltered at −2 kb (Fig. 7h). In contrast, the H3K56Ac level was upregulated about twofold at −2 kb but not at the TSS of *Txnip* (Fig. 7i). These results suggest that SIRT6 deficiency resulted in a more open chromatin state around the *Txnip* promoter region. Since we did not find that SIRT6 was present at the −2 kb region of the *Txnip* gene (Fig. 7a), it is currently unclear whether this inconsistency was due to low ChIP signal of SIRT6 when chromatins were prepared from a limited number of cells [23]. To further confirm the influence of these changes on *Txnip* gene transcription, we performed phospho-Ser5-RNA polymerase II ChIP. As expected, active RNA polymerase II intensity in the mutant islets was twofold higher than in control islets at both the TSS and −2 kb (Fig. 7j). Taken together, these findings suggest that SIRT6 directly suppresses *Txnip* expression in beta cells through deacetylation of H3K9 and H3K56 at the promoter region of *Txnip*.

Long-term deletion of *Sirt6* in beta cells induces susceptibility to STZ While investigating the impact of *Sirt6* knockout on H3 lysine acetylation, we serendipitously found that the increased H3K9Ac and H3K56Ac levels in islets from *Sirt6* BKO mice were more evident when they were from mice at a much later

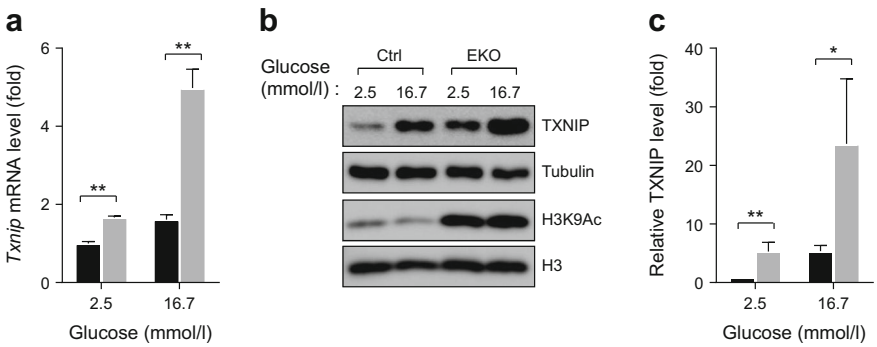

Fig. 6 SIRT6 regulates both basal and glucose-induced *Txnip* transcription. (**a**) RT-qPCR analysis of *Txnip* mRNA in islets isolated from 3-month-old control (*Sirt6*$^{f/f}$) and *Sirt6* EKO mice in response to treatment for 1 h with 16.7 mmol/l glucose ($n = 3$ or 4). (**b**, **c**) Immunoblots (**b**) and quantification (**c**) of TXNIP and H3K9Ac levels in islets treated as in (**a**). Black bars, control mouse islets; grey bars, *Sirt6* EKO mouse islets. Data are expressed as means ± SEM. *$p < 0.05$ and **$p < 0.01$ for indicated comparisons

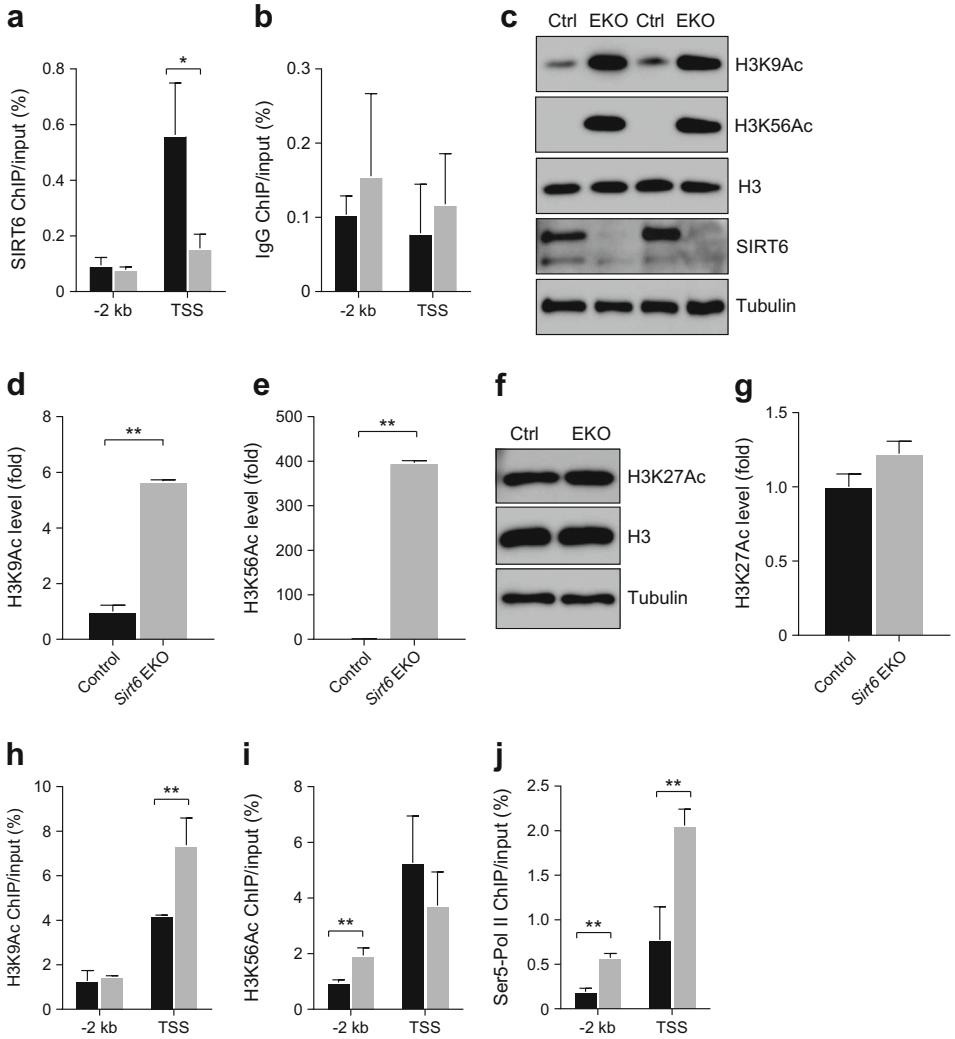

Fig. 7 SIRT6 regulates TXNIP through H3K9Ac and H3K56Ac deacetylation. (**a**) ChIP assay of SIRT6 at 2 kb upstream of TSS (−2 kb) and at the TSS of the *Txnip* gene. Islets pooled from four or five mice were used, the result was the average of three experiments; error bars represent SEM. (**b**) ChIP assay of IgG at −2 kb and the TSS of the *Txnip* gene. (**c**–**e**) Representative immunoblots (**c**) and quantification (**d**, **e**) of H3K9Ac and H3K56Ac in islets from 3-month-old control (Ctrl, $Sirt6^{f/f}$) and *Sirt6* EKO mice ($n = 6$). (**f**, **g**) Representative immunoblots (**f**) and quantification (**g**) of H3K27Ac in islets from 3-month-old control and *Sirt6* EKO mice ($n = 6$). (**h**–**j**) ChIP assays of H3K9Ac (**h**), H3K56Ac (**i**) and Ser5-polymerase (Pol) II (**j**) at −2 kb and the TSS of the *Txnip* gene in islets isolated from control and *Sirt6* EKO mice. Three biological repeats were used for (**d**) and (**e**); for (**f**), islets pooled from four or five mice were used. The result was the average of three experiments; error bars represent SEM. Black bars, control mouse islets; grey bars, *Sirt6* EKO mouse islets. Data are expressed as means ± SEM, unless stated otherwise. $*p < 0.05$ and $**p < 0.01$ for indicated comparisons

time point post-tamoxifen treatment (ESM Fig. 6a). This was correlated with an increase in *Txnip* mRNA level (ESM Fig. 6b). The time-dependent increase in H3K9Ac, H3K56Ac and TXNIP levels post-tamoxifen treatment or with age were reproduced in both the BKO and EKO model (ESM Fig. 6c and Fig. 8a), excluding the possibility that this was due to prolonged tamoxifen-induced gene recombination, as reported previously [36]. Together, these results suggest that loss of *Sirt6* leads to a progressive accumulation of H3K9Ac and H3K56Ac and sustained upregulation of TXNIP in beta cells, which is likely to be the molecular basis of the time-dependent worsening of glucose intolerance in the SIRT6-deficient mice.

As TXNIP expression is associated with beta cell apoptosis [28], we next examined whether TXNIP accumulation affects the viability of SIRT6-deficient beta cells, especially in older *Sirt6*-knockout mice. Of note, the islet mass of 11-month-old *Sir6* EKO mice did not differ appreciably from that of control mice (Fig. 8b, c), indicating that upregulation of TXNIP in SIRT6-deficient beta cells did not cause spontaneous cell death. Next, we tested whether SIRT6-deficient beta cells are sensitive to STZ [37], a genotoxic agent. As STZ selectively acts on beta cells, we directly treated the mice with STZ. Interestingly, the older SIRT6-deficient mice (>6 month old) showed a more dramatic response to STZ treatment

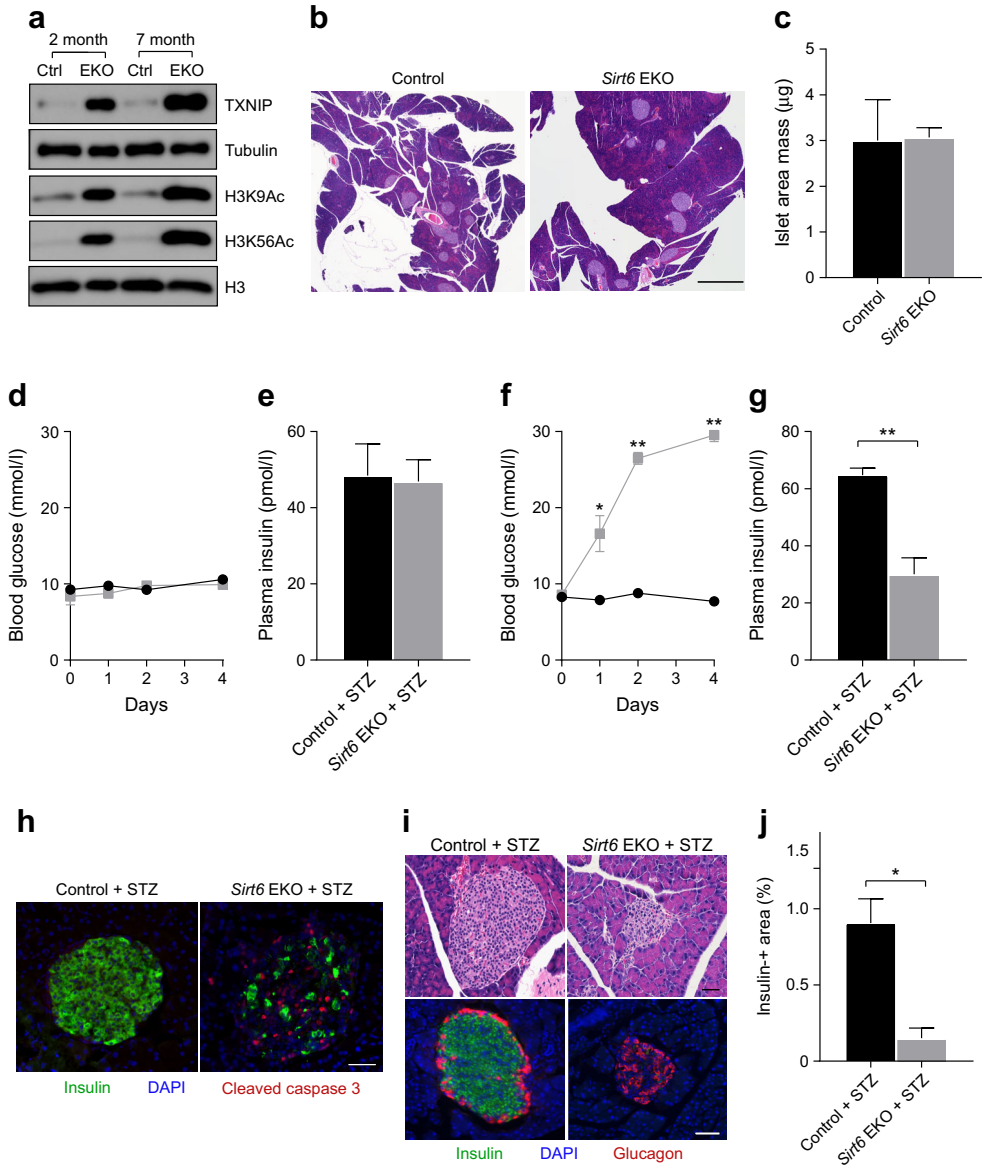

Fig. 8 Long-term deletion of *Sirt6* in beta cells induces susceptibility to STZ. (**a**) Immunoblots of TXNIP, H3K9Ac and H3K56Ac in islets isolated from 2-month-old and 7-month-old control (Ctrl, $Sirt6^{f/f}$) and *Sirt6* EKO mice. (**b**) Representative H&E staining of pancreases from 11-month-old control and *Sirt6* EKO mice. Scale bar, 1 mm. (**c**) Quantification of the mass of the islet area in (**b**). (**d**) Blood glucose levels in 2-month-old male control and *Sirt6* EKO mice after a single STZ treatment (75 mg/kg). (**e**) Plasma insulin levels in 2-month-old male control and *Sirt6* EKO mice 2 days after a single STZ treatment. (**f**) Blood glucose levels in 7-month-old control and *Sirt6* EKO mice after a single STZ treatment (75 mg/kg) ($n = 6$). (**g**) Plasma insulin levels of 7-month-old control and *Sirt6* EKO mice 2 days after a single STZ treatment. (**h**) Immunostaining of pancreases from 7-month-old control and *Sirt6* EKO mice 2 days after a single STZ treatment. Green, anti-insulin; red, anti-cleaved caspase 3; blue, DAPI. Scale bar, 50 µm. (**i**) Representative H&E staining and immunostaining of pancreases from 7-month-old control and *Sirt6* EKO mice 4 days after a single STZ treatment. Green, anti-insulin; red, anti-glucagon; blue, DAPI. Scale bar, 50 µm. (**j**) Quantification of the insulin-positive area of 7-month-old control and *Sirt6* EKO mice 4 days after a single STZ treatment. Black bars and circles, control mice; grey bars and squares, *Sirt6* EKO mice. Data are expressed as means ± SEM ($n = 3$ or 4, unless stated otherwise). *$p < 0.05$ and **$p < 0.01$ vs control condition or for indicated comparisons

than the older control mice or younger mice (2 months old) in both EKO and BKO models (Fig. 8d–g and ESM Fig. 6d, e). Upon a single injection of STZ (75 mg/kg for *Sirt6* EKO mice and 140 mg/kg for *Sirt6* BKO mice), all older SIRT6-deficient mice displayed hyperglycaemia (blood glucose level >16 mmol/l) after 2 days, due to insulin insufficiency (Fig. 8g). Consistent with this finding, a massive beta cell loss was observed within 2 days of STZ treatment of older SIRT6-deficient mice, as demonstrated by cleaved caspase 3, H&E and insulin staining (Fig. 8h–j). These findings suggest that long-term deficiency of SIRT6 in beta cells affects beta cell survival, which is correlated with sustained upregulation of TXNIP.

Discussion

In this study, we reported that SIRT6 is not required for beta cell development but is essential for insulin secretion function of beta cells. Our unbiased gene expression profiling studies identified *Txnip* as a SIRT6 target. Concurrently, inhibition of TXNIP by verapamil could partially rescue the insulin secretion defect in *Sirt6*-knockout mice. In addition, we showed that SIRT6 directly suppresses *Txnip* expression by catalysing the deacetylation of H3K9 and H3K56 at the *Txnip* promoter region. Finally, we uncovered an unanticipated time-dependent increase in H3K9Ac, H3K56Ac and TXNIP levels in SIRT6 null beta cells, which correlates with a worsened insulin secretion defect and leads to increased susceptibility to the diabetogenic agent STZ. These findings clearly highlight the important roles of SIRT6 histone deacetylation activity in supporting beta cell function and viability (Fig. 9).

Glucose-stimulated insulin secretion in beta cells is a complex process that requires coupling of cellular metabolism with ATP-sensitive potassium channels and subsequent activation of voltage-dependent calcium channel-mediated $^{Ca2+}$ influx [1]. Xiong et al observed a decrease in cellular ATP levels, accumulation of damaged mitochondria, reduction in electron transport chain protein levels and impaired Ca2+ influx in SIRT6-deficient beta cells [25]. However, they did not identify the molecular mechanism linking these phenotypic findings with loss of SIRT6. We found that expression of TXNIP is upregulated in *Sirt6* null mouse islets and that reducing TXNIP level by verapamil was able to partially restore the insulin secretion and largely rescue the glucose intolerance in mice. In agreement with our findings, TXNIP expression is negatively correlated with glucose-stimulated insulin secretion capacity in beta cells [29–31]. Importantly, Yoshihara et al demonstrated that genetic disruption of *Txnip* enhanced glucose-stimulated insulin secretion, whereas overexpression of TXNIP in INS1 cells in the first 48 h attenuated this process, likely through an effect on mitochondrial ATP production [29]. Although *Ucp2* was identified as a TXNIP transcriptional target in their study and presumably caused the reduction in cellular ATP levels [29], we did not detect significant changes in *Ucp2* mRNA levels in our model. In addition, Song et al showed that loss of SIRT6 in beta cells stimulated transcriptional repression activity of forkhead box O1 and led to downregulation of its two targets, *Pdx1* and *Glut2* (also known as *Slc2a2*) [26]. However, expression levels of *Pdx1* and *Glut2* were not changed in either of our models. These discrepancies could be attributed to differences in mouse genetic background and methodologies used in these molecular characterisations. However, it is still unclear how TXNIP affects insulin secretion in our model.

Verapamil is a calcium antagonist and has been shown to inhibit insulin release in islets isolated from rodents [38, 39]. However, verapamil treatment has no significant effect on either glucose tolerance or insulin secretion in vivo [39, 40], consistent with our observations. Thus, our finding that oral verapamil treatment improved glucose tolerance and insulin secretion is likely mediated by *Txnip* suppression. As verapamil inhibits *Txnip* through an indirect calcium-dependent calcineurin pathway [32], genetically or pharmacologically attenuating TXNIP activity would be necessary for future

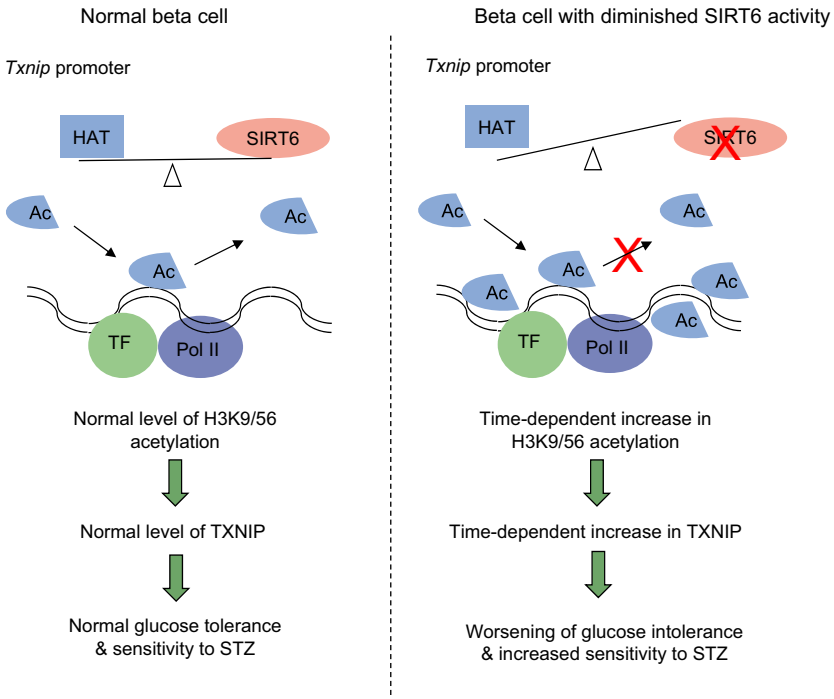

Fig. 9 Diagram depicting a proposed role for SIRT6 supporting beta cell function and survival through inhibition of *Txnip* transcription. Ac, acetylation; Pol II, RNA polymerase II; TF, transcription factor

studies to more precisely dissect the contribution of TXNIP to the SIRT6-deficient mouse phenotype.

TXNIP mainly functions as an inhibitor of thioredoxin by antagonising its scavenger effect on ROS [28]. Thus, upregulation of TXNIP is implicated in glucose-, endoplasmic reticulum (ER) stress- and STZ-induced cell death [28]. We found that upregulation of TXNIP in SIRT6-deficient beta cells did not cause spontaneous cell death. Consistent with this finding, SIRT6 deficiency did not induce ROS accumulation in islets (data not shown). However, several genes in the oxidation–reduction pathway including *Nqo1*, *Gstm7* and *Dusp26* were significantly upregulated in the islets from *Sirt6* EKO but not *Sirt6* BKO mice (GSE104161). Whether this is a compensatory response to TXNIP-induced oxidative stress or the direct consequence of SIRT6 deficiency requires further investigation. We speculate that the progressive upregulation of TXNIP in SIRT6-deficient beta cells induces a gradual increase in ROS that the cells can cope with by upregulating the genes in the oxidation–reduction pathways.

Genetic background of mice is a contributing factor to phenotypic variation, including metabolic traits and the response to STZ [37, 41]. However, the severity and time-dependent progression of the functional defects in our models, as well as the similarity between our EKO and BKO model, strongly suggest that these phenotypes are independent of mouse genetic background. Multiple studies have reported that the transgene-driven human growth hormone expression in the MIP-CreER mouse strain has a profound effect on gene expression and beta cell integrity [19, 42, 43]. Specifically, islets in MIP1-CreER mice are less sensitive to the cytotoxic effect of STZ [19]. To avoid this potential confounding factor, mice carrying the Cre transgene were used as controls throughout the BKO study (ESM Fig. 4).

In conclusion, our study demonstrates that SIRT6 is required for glucose-stimulated insulin secretion and cell survival in beta cells, partially via suppression of *Txnip* transcription. As defective insulin secretion and loss of beta cell mass are the main culprits of type 2 diabetes [1], our findings raise the possibility that preserving SIRT6 activity and expression could be beneficial in improving beta cell function and maintaining beta cell mass in individuals with impaired glucose tolerance or type 2 diabetes.

Acknowledgements We thank Y. Liu (Department of Cell Systems & Anatomy, Greehey Children's Cancer Research Institute, University of Texas Health Science Centre at San Antonio, USA) for assistance in analysing the RNA-Seq data and thank C. Cervantes (Department of Pharmacology, University of Texas Health Science Centre at San Antonio, USA) and C. Dong (Biochemistry Molecular Biology, Indiana University, USA) for critical reading of the manuscript.

Data availability Sequence data have been deposited in the NIH Gene Expression Omnibus (GEO) with the accession code GSE104161. All other remaining data are available within the article and ESM files or are available from the authors on request.

Funding PW and KX are CPRIT Scholars and are supported by the Cancer Prevention and Research Institute of Texas. This work was supported by grants from the NIH (R01-DK80157 and R01-DK089229) and the American Diabetes Association to NM. This research also was supported by the San Antonio Nathan Shock Centre of Excellence in Aging Biology (P30 AG013319) and San Antonio Claude D. Pepper Older Americans Independence Centre (P30 AG044271).

Duality of interest The authors declare that there is no duality of interest associated with this manuscript.

Contribution statement KQ and PW were responsible for designing the experiments. KQ, NZ, ZZ, MN, ZXZ and JL were responsible for acquisition of data. KQ, NZ, KX, NM and PW analysed and interpreted data. KQ drafted the manuscript. All authors critically revised the manuscript and approved the final version. PW is the guarantor of this work.

References

1. Ashcroft FM, Rorsman P (2012) Diabetes mellitus and the beta cell: the last ten years. Cell 148:1160–1171
2. Zaccardi F, Webb DR, Yates T, Davies MJ (2016) Pathophysiology of type 1 and type 2 diabetes mellitus: a 90-year perspective. Postgrad Med J 92:63–69
3. Xie R, Carrano AC, Sander M (2015) A systems view of epigenetic networks regulating pancreas development and beta-cell function. Wiley Interdiscip Rev Syst Biol Med 7:1–11
4. Bernstein D, Golson ML, Kaestner KH (2017) Epigenetic control of β-cell function and failure. Diabetes Res Clin Pract 123:24–36
5. Arguelles AO, Meruvu S, Bowman JD, Choudhury M (2016) Are epigenetic drugs for diabetes and obesity at our door step? Drug Discov Today 21:499–509
6. Haberland M, Montgomery RL, Olson EN (2009) The many roles of histone deacetylases in development and physiology: implications for disease and therapy. Nat Rev Genet 10:32–42
7. Lee KK, Workman JL (2007) Histone acetyltransferase complexes: one size doesn't fit all. Nat Rev Mol Cell Biol 8:284–295
8. Remsberg JR, Ediger BN, Ho WY et al (2017) Deletion of histone deacetylase 3 in adult beta cells improves glucose tolerance via increased insulin secretion. Mol Metab 6:30–37
9. Chang HC, Guarente L (2014) SIRT1 and other sirtuins in metabolism. Trends Endocrinol Metab 25:138–145
10. Imai S, Guarente L (2014) NAD+ and sirtuins in aging and disease. Trends Cell Biol 24:464–471
11. Michishita E, McCord RA, Berber E et al (2008) SIRT6 is a histone H3 lysine 9 deacetylase that modulates telomeric chromatin. Nature 452:492–496
12. Yang B, Zwaans BM, Eckersdorff M, Lombard DB (2009) The sirtuin SIRT6 deacetylates H3 K56Ac in vivo to promote genomic stability. Cell Cycle 8:2662–2663
13. Tasselli L, Xi Y, Zheng W et al (2016) SIRT6 deacetylates H3K18ac at pericentric chromatin to prevent mitotic errors and cellular senescence. Nat Struct Mol Biol 23:434–440
14. Tasselli L, Zheng W, Chua KF (2017) SIRT6: novel mechanisms and links to aging and disease. Trends Endocrinol Metab 28:168–185
15. Kim HS, Xiao C, Wang RH et al (2010) Hepatic-specific disruption of SIRT6 in mice results in fatty liver formation due to enhanced glycolysis and triglyceride synthesis. Cell Metab 12:224–236
16. Schonhoff SE, Giel-Moloney M, Leiter AB (2004) Neurogenin 3-expressing progenitor cells in the gastrointestinal tract differentiate into both endocrine and non-endocrine cell types. Dev Biol 270: 443–454

17. Wicksteed B, Brissova M, Yan W et al (2010) Conditional gene targeting in mouse pancreatic ss-cells: analysis of ectopic Cre transgene expression in the brain. Diabetes 59:3090–3098
18. Pan H, Qin K, Guo Z et al (2014) Negative elongation factor controls energy homeostasis in cardiomyocytes. Cell Rep 7:79–85
19. Oropeza D, Jouvet N, Budry L et al (2015) Phenotypic characterization of MIP-CreERT1Lphi mice with transgene-driven islet expression of human growth hormone. Diabetes 64:3798–3807
20. Zhang J, Zhang N, Liu M et al (2012) Disruption of growth factor receptor-binding protein 10 in the pancreas enhances beta-cell proliferation and protects mice from streptozotocin-induced beta-cell apoptosis. Diabetes 61:3189–3198
21. Neuman JC, Truchan NA, Joseph JW, Kimple ME (2014) A method for mouse pancreatic islet isolation and intracellular cAMP determination. J Vis Exp e50374
22. Benitez CM, Qu K, Sugiyama T et al (2014) An integrated cell purification and genomics strategy reveals multiple regulators of pancreas development. PLoS Genet 10:e1004645
23. Dahl JA, Collas P (2008) A rapid micro chromatin immunoprecipitation assay (microChIP). Nat Protoc 3:1032–1045
24. Goodyer WR, Gu X, Liu Y, Bottino R, Crabtree GR, Kim SK (2012) Neonatal β cell development in mice and humans is regulated by calcineurin/NFAT. Dev Cell 23:21–34
25. Xiong X, Wang G, Tao R et al (2016) Sirtuin 6 regulates glucose-stimulated insulin secretion in mouse pancreatic beta cells. Diabetologia 59:151–160
26. Song MY, Wang J, Ka SO, Bae EJ, Park BH (2016) Insulin secretion impairment in Sirt6 knockout pancreatic β cells is mediated by suppression of the FoxO1-Pdx1-Glut2 pathway. Sci Rep 6:30321
27. Ayala JE, Samuel VT, Morton GJ et al (2010) Standard operating procedures for describing and performing metabolic tests of glucose homeostasis in mice. Dis Model Mech 3:525–534
28. Shalev A (2014) Minireview: thioredoxin-interacting protein: regulation and function in the pancreatic β-cell. Mol Endocrinol 28:1211–1220
29. Yoshihara E, Fujimoto S, Inagaki N et al (2010) Disruption of TBP-2 ameliorates insulin sensitivity and secretion without affecting obesity. Nat Commun 1:127
30. Rani S, Mehta JP, Barron N et al (2010) Decreasing Txnip mRNA and protein levels in pancreatic MIN6 cells reduces reactive oxygen species and restores glucose regulated insulin secretion. Cell Physiol Biochem 25:667–674
31. Luo Y, He F, Hu L et al (2014) Transcription factor Ets1 regulates expression of thioredoxin-interacting protein and inhibits insulin secretion in pancreatic beta-cells. PLoS One 9:e99049
32. Xu G, Chen J, Jing G, Shalev A (2012) Preventing β-cell loss and diabetes with calcium channel blockers. Diabetes 61:848–856
33. De Marinis Y, Cai M, Bompada P et al (2016) Epigenetic regulation of the thioredoxin-interacting protein (TXNIP) gene by hyperglycemia in kidney. Kidney Int 89:342–353
34. Yu FX, Luo Y (2009) Tandem ChoRE and CCAAT motifs and associated factors regulate Txnip expression in response to glucose or adenosine-containing molecules. PLoS One 4:e8397
35. Etchegaray JP, Chavez L, Huang Y et al (2015) The histone deacetylase SIRT6 controls embryonic stem cell fate via TET-mediated production of 5-hydroxymethylcytosine. Nat Cell Biol 17:545–557
36. Reinert RB, Kantz J, Misfeldt AA et al (2012) Tamoxifen-induced Cre-loxP recombination is prolonged in pancreatic islets of adult mice. PLoS One 7:e33529
37. Deeds MC, Anderson JM, Armstrong AS et al (2011) Single dose streptozotocin-induced diabetes: considerations for study design in islet transplantation models. Lab Anim 45:131–140
38. Devis G, Somers G, Van Obberghen E, Malaisse WJ (1975) Calcium antagonists and islet function. I. Inhibition of insulin release by verapamil. Diabetes 24:247–251
39. Semple CG, Smith M, Furman BL (1988) Inhibition of glucose-induced insulin secretion by calcium channel blocking drugs in-vitro but not in-vivo in the rat. J Pharm Pharmacol 40:22–26
40. Semple CG, Thomson JA, Beastall GH, Lorimer AR (1983) Oral verapamil does not affect glucose tolerance in non-diabetics. Br J Clin Pharmacol 15:570–571
41. Champy MF, Selloum M, Zeitler V et al (2008) Genetic background determines metabolic phenotypes in the mouse. Mamm Genome 19:318–331
42. Brouwers B, de Faudeur G, Osipovich AB et al (2014) Impaired islet function in commonly used transgenic mouse lines due to human growth hormone minigene expression. Cell Metab 20: 979–990
43. Carboneau BA, Le TD, Dunn JC, Gannon M (2016) Unexpected effects of the MIP-CreER transgene and tamoxifen on β-cell growth in C57Bl6/J male mice. Physiological reports 4:e12863